Applied Surface Science 254 (2008) 6257–6260

Contents lists available at ScienceDirect

Applied Surface Science

journal homepage: www.elsevier.com/locate/apsusc

Carrier gas effects on the SiGe quantum dots formation

C.-H. Lee [a], C.-Y. Yu [a], C.M. Lin [a], C.W. Liu [a,b,*], H. Lin [c], W.-H. Chang [c]

[a] Department of Electrical Engineering and Graduate Institute of Electronics Engineering, National Taiwan University, Taipei, Taiwan, ROC
[b] National Nano Device Laboratories, Hsinchu, Taiwan, ROC
[c] Department of Electrophysics, National Chiao Tung University, Hsinchu, Taiwan, ROC

ARTICLE INFO

Article history:
Available online 18 March 2008

PACS:
68.65.Ac
68.65.Hb
68.55.-a
66.30.-h

Keywords:
Carrier gas effect
SiGe quantum dot
Hydrogen passivation
Surface mobility
UHVCVD

ABSTRACT

SiGe quantum dots (QDs) grown by ultra-high vacuum chemical vapor deposition using H_2 and He carrier gases are investigated and compared. SiGe QDs using He carrier gas have smaller dot size with a better uniformity in terms of dot height and dot base as compared to the H_2 carrier gas. There is a higher Ge composition and less compressive strain in the SiGe QDs grown in He than in H_2 as measured by Raman spectroscopy. The Ge content is higher for He growth than H_2 growth due to hydrogen induced Si segregation and the lower interdiffusivity caused by the more strain relaxation in the He-grown SiGe dots. The photoluminescence also confirms more compressive strain for H_2 growth than He growth. Hydrogen passivation and Ge–H cluster formation play an important role in the QDs growth.

1. Introduction

Self-assembled SiGe quantum dots (QDs) have attracted much interest in the potential applications in nanoelectronics and optoelectronics recently. To meet the requirement of device applications, size and shape uniformity are the two most important parameters to be considered. Influences of temperature [1], wetting-layer growth [2], and Si capping [3] on dot size and dot shape have been reported in previous works. Carrier gases such as He [4], H_2 [5], and N_2 [6], have been used in the process to control the partial pressure of precursors. However, the comparison of different carrier gases was not reported yet. In this work, morphologies of SiGe QDs grown in He and H_2 were characterized by atomic force microscopy (AFM) and high-angle annular dark-field scanning transmission electron microscopy (HAADF-STEM). Strain relaxation and Ge composition were investigated through Raman spectroscopy, low temperature photoluminescence (PL) measurement, and energy dispersive X-ray spectroscopy (EDS). Moreover, a simple epitaxial model is proposed for He and H_2 growth.

2. Experimental procedures

SiGe QDs were grown by ultra-high vacuum chemical vapor deposition (UHV/CVD) at 600 °C. The base pressure of our UHVCVD system was ultra-high vacuum of 10^{-9} Torr. Pure silane (SiH_4) and germane (GeH_4) were used as reactant gases, and the gas flow ratio of GeH_4 and carrier gases (H_2 and He) was fixed at 100 sccm/100 sccm for QDs growth. Before the epitaxial growth, Si wafers were dipped in 10% HF solution to remove the native oxide. No SiH_4 was used during QDs growth. Due to the Si/Ge interdiffusion at 600 °C, Ge layers transformed into SiGe alloys. After the deposition of ~60-nm-thick Si buffer layer using the SiH_4 flow rate of 100 sccm, 1-layer and 5-layers QDs were grown. Finally, a ~15-nm Si cap layer using SiH_4 flow rate of 100 sccm was grown on top of the SiGe QDs layer to avoid oxidation of the SiGe surface. Note that there were no carrier gases during the Si buffer layer and Si cap layer growth. In this work, we used pure germane for the reactant gas instead of dilute germane in He or H_2, and the gas flow maintained at 100 sccm for QDs growth. The Ge partial pressure should be the same for H_2 and He growth. For the SiGe quantum well growth at 500 °C, the thickness of SiGe film is ~3 nm for both He growth and H_2 growth. The carrier gas effect on the Ge growth rate seems similar in this work. Variations in Ge composition, dot density and strain are due to the surface effect instead of the Ge partial pressure (dose).

* Corresponding author at: Department of Electrical Engineering and Graduate Institute of Electronics Engineering, National Taiwan University, No. 1, Sec. 4, Roosevelt Road, Taipei 10617, Taiwan, ROC. Tel.: +886 2 23635251x515; fax: +886 2 23638247.
E-mail address: chee@cc.ee.ntu.edu.tw (C.W. Liu).

0169-4332/$ – see front matter © 2008 Elsevier B.V. All rights reserved.
doi:10.1016/j.apsusc.2008.02.152

3. Results and discussion

Morphologies of 1-layer SiGe QDs without Si capping layer grown in He and in H_2 have been observed by AFM (Fig. 1). Average dot heights are 10 and 12 nm for He and H_2 growth, while average dot bases are 88 and 89 nm for He and H_2 growth, respectively. Dot densities are similar ($\sim 1.1 \times 10^{10}$ cm^{-2}) for He-grown sample and H_2-grown sample. The average dot height indicates that H_2-grown sample can have slightly taller dots (12 nm height) than He-grown sample (10 nm height) measured by AFM. The HAADF-STEM also shows the similar trend. Dot height distribution (Fig. 2) and dot base distribution (Fig. 3) are different for H_2 growth and He growth. For H_2-grown sample, the bimodality is clearly evidenced in H_2 growth for dot height distribution (Fig. 2(b)), and a broad distribution is observed for dot base (Fig. 3). Standard deviations of dot height are 3.2 and 4.4 nm for He growth and H_2 growth, respectively, and those of dot base are 29 and 41 nm for He growth and H_2 growth, respectively. QDs grown in He have better uniformity than in H_2. Different morphologies are also found through HAADF-STEM images. The scanning transmission electron microscopy of 5-layers QDs grown in He and H_2 are shown in Fig. 4(a) and (b), respectively. The thickness of the Si layer between the SiGe QDs layers is $\sim$60 nm. H_2 carrier gas creates taller dots than He carrier gas, consistent with AFM results.

Raman spectra of 5-layers SiGe QDs grown in He and H_2 with 488 nm laser excitation are shown in Fig. 5 with the resolution of 0.2 cm^{-1}. Besides strong bulk Si signal at 520 cm^{-1}, the Si–Ge 2TA phonon, Ge–Ge phonon, and Si–Ge phonon of dots were also observed. For the peak at $\sim$417 cm^{-1}, QDs contribute more intensity of the Raman spectra than wetting layers. The sample with wetting layers only has very weak intensity at $\sim$417 cm^{-1}. The Si–Ge phonon peak ($\sim$417 cm^{-1}) is sensitive to both the strain

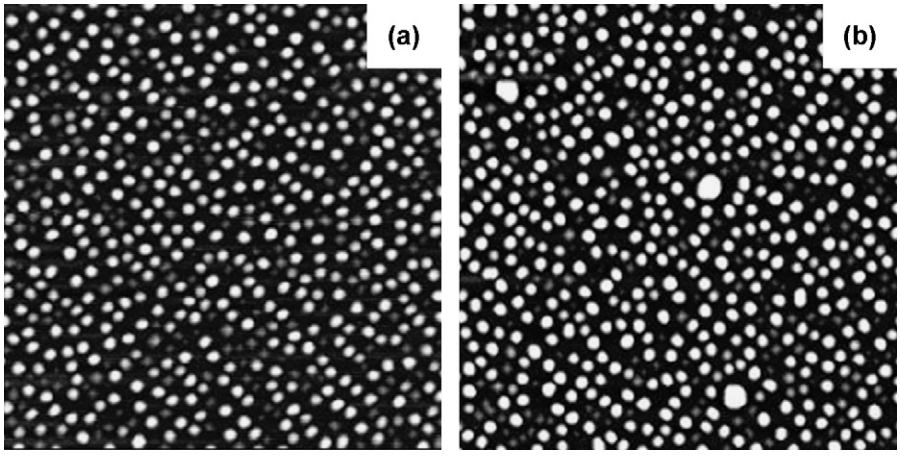

Fig. 1. The 2.5 μm × 2.5 μm AFM image of SiGe QDs grown in different carrier gases: (a) He and (b) H_2.

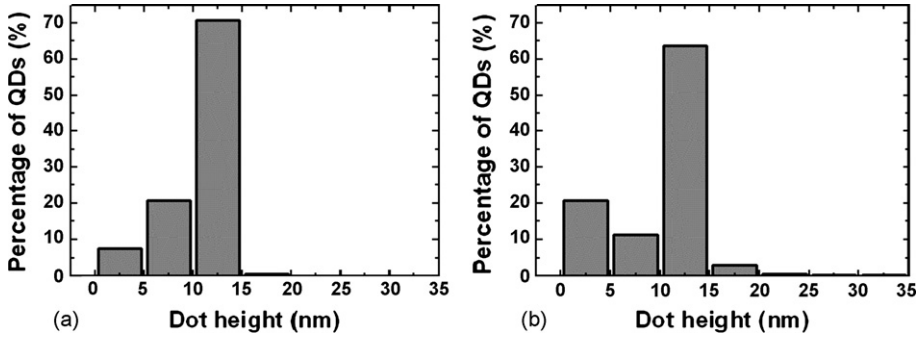

Fig. 2. The dot height distribution of SiGe QDs grown in (a) He and (b) H_2. The bimodality is clearly evidenced in H_2 growth.

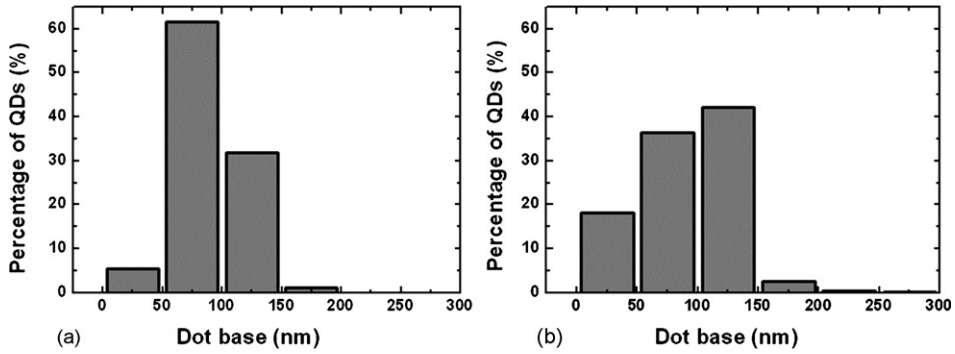

Fig. 3. The dot base distribution of SiGe QDs grown in (a) He and (b) H_2.

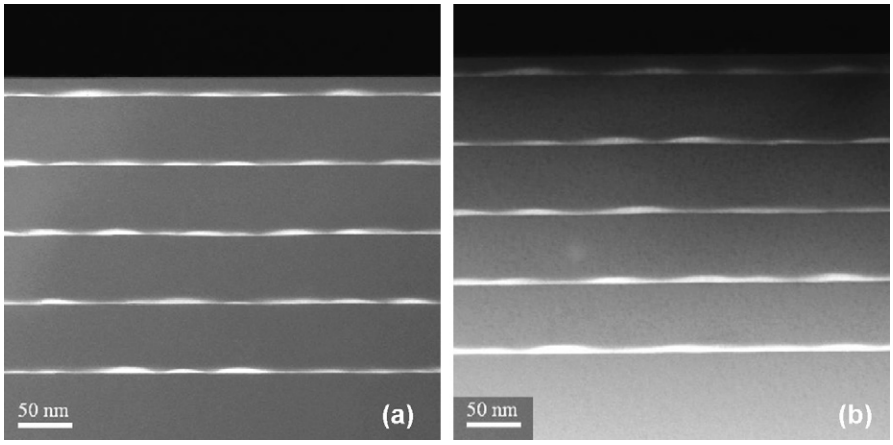

Fig. 4. The HAADF-STEM images of the regular regions of QDs grown in (a) He and (b) H_2.

and Ge composition [7]. Both more compressive strain and higher Ge content increase the wave number of this peak. The Si–Ge 2TA phonon peak (at ~220 cm^{-1}) is sensitive to only the Ge concentration [8,9]. Wave numbers of 2TA mode are ~222 and ~223 cm^{-1} for He growth and H_2 growth, respectively. Note that the ~1 cm^{-1} Raman shift between He-grown and H_2-grown QDs is well beyond the resolution (0.2 cm^{-1}) of the Raman measurement. The ~1 cm^{-1} lower in wave number of 2TA mode indicates the average Ge concentration of He-grown SiGe layers is ~2% higher than H_2-grown layers [10]. The ~2% larger Ge content leads to a ~0.6 cm^{-1} shift of the Raman peak at ~417 cm^{-1} [11] if lattice strain are the same in He-grown and H_2-grown samples. However, wave numbers of Si–Ge phonon peaks are both at ~416.5 cm^{-1} for He and H_2 growth. This result indicates that He-grown QDs have less strain (more relaxation) than H_2-grown QDs. The larger Ge concentration in SiGe QDs grown in He is partly attributed to the highly relaxed nature of the dots. Note that H_2 carrier gas can create slightly taller dots than He carrier gas. The smaller dot height in He-grown sample, which corresponds to a smaller contact angle, leads to more relaxation than H_2-grown sample due to the decrease of strain energy [12].

Higher Ge content suggested in the Raman measurement is due to suppressed Ge/Si interdiffusion in He-grown QDs. The stronger Si/Ge interdiffusion due to larger compressive strain [13] in H_2-grown sample leads to less Ge content, which is consistent with the conclusions from Raman measurement. H_2 carrier gas, which increases Si segregation during QDs growth [14] can also be responsible for the smaller Ge composition in H_2-grown sample. Note that the Ge concentration difference between He-grown and H_2-grown samples cannot be resolved by EDS. Fig. 6 shows the low temperature (10 K) PL measurement of 5-layers QDs with He and H_2 carrier gases. The PL emission peak of He-grown sample is ~13 meV higher than that of H_2-grown sample. Ge concentration and strain might be responsible for the emission peak shift. For the effect of Ge content, the emission peak of He-grown sample should be ~6 meV lower than that of H_2-grown sample due to higher Ge content [15]. However, this is not consistent with the experimental measurement. Strain of H_2-grown sample is ~0.11% higher than that of He-grown sample based on the Raman result [8]. The emission peak of the He-grown sample would be ~12 meV higher than that of H_2-grown sample due to less compressive strain in QDs. Considering the effect of Ge content and strain simultaneously, the net emission peak shift is ~6 meV. He-grown sample has higher PL emission peak energy than H_2-grown sample, which agrees with the experimental data qualitatively. The error of quantitative analysis (6 vs. 13 meV) is probably due to some measurement error, but is not fully understood.

Carrier gas effect plays an important role in the QDs growth. Fig. 7 shows a simple growth model for H_2 and He growth. For H_2 carrier gas, the Si surface is passivated by hydrogen due to the adsorption of H_2 from the environment [16]. Hydrogen passivation can block the surface sites for dissociative adsorption of germane [17]. H_2-rich environment also enhances the Ge–H cluster formation, which increases Ge surface mobility [18] and strengthens surface diffusion. Ge atoms can diffuse on the surface and assemble with other Ge atoms which have been already adsorbed on surface sites. Never-

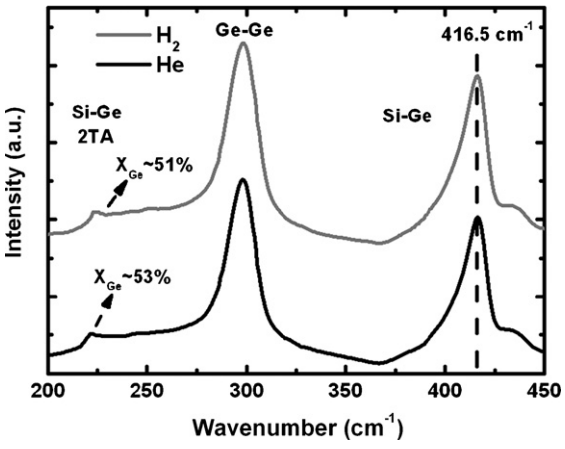

Fig. 5. The Raman spectra of SiGe QDs grown in He and H_2.

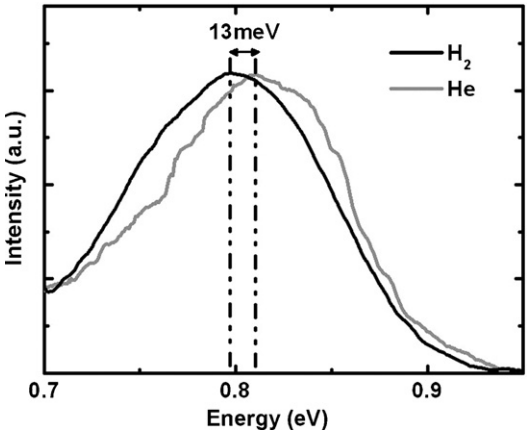

Fig. 6. The PL spectrum of the SiGe dots grown in He and H_2. The ~13 meV variation of the emission peak is caused by the difference in compressive strain.

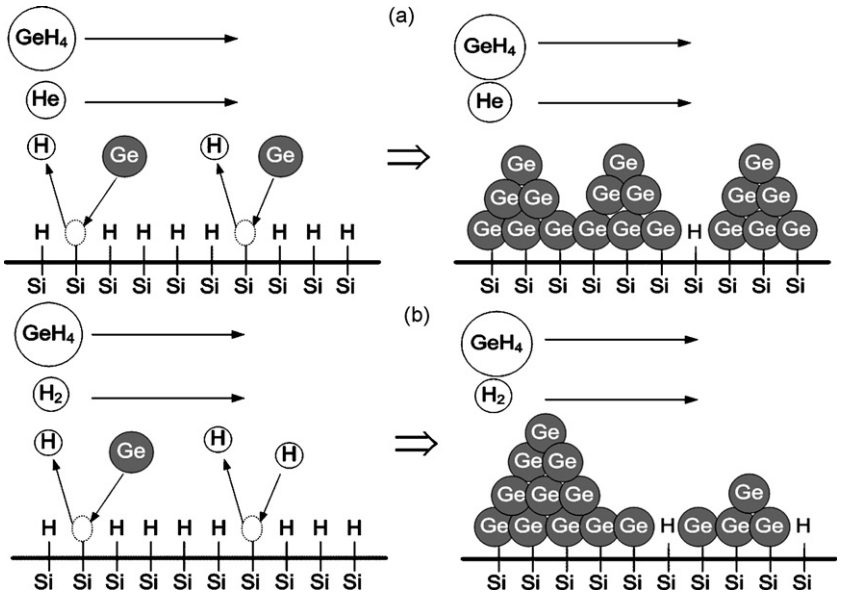

Fig. 7. The growth model of SiGe dots grown in (a) He and (b) H_2. The major difference is the hydrogen induced H-passivation on the surface.

theless, for He carrier gas, hydrogen passivation decreases since there are no H_2 in the environment. The He carrier gas flow can take away the hydrogen which is desorbed on the surface, and surface mobility can also reduce due to the reduction of Ge–H cluster. Therefore, H_2 carrier gas creates taller dots and worse uniformity in dots distribution than He carrier gas.

4. Conclusion

In conclusion, morphologies, compressive strain and Ge composition of QDs in He and in H_2 carrier gases are studied. The He growth has a smaller dot size and a better uniformity in dots height and base width distribution than H_2 growth. Raman results show higher Ge concentration and more relaxation in 5-layers QDs layer grown in He as compared to those grown in H_2 carrier gas. Higher dot density for He growth leads to a larger strain relaxation in SiGe layer as compared to H_2 growth. Hydrogen induced Si segregation and slower Si/Ge interdiffusion due to smaller strain are responsible for the lower Ge content in He-grown sample. PL spectra also confirm smaller compressive in He-grown sample. Hydrogen passivation during the process and Ge–H cluster formation should be responsible for the difference between He growth and H_2 growth.

Acknowledgements

The authors would like to acknowledge Dr. Yung-Hui Yeh and Mr. H. T. Chen at the DTC/ITRI for the Raman measurement, and D. J. Lockwood, J. -M. Baribeau and X. Wu at the National Research Council of Canada for the HAADF-STEM measurement. This work was supported by National Nano Device Laboratories and National Science Council of ROC under contract no. 95-2221-E-002-370.

Reference

[1] G. Jin, J.L. Liu, K.L. Wang, Appl. Phys. Lett. 83 (2003) 2847.
[2] H.J. Kim, Y.H. Xie, Appl. Phys. Lett. 79 (2001) 263.
[3] Y.Q. Wu, F.H. Li, J. Cui, J.H. Lin, R. Wu, J. Qin, C.Y. Zhu, Y.L. Fan, X.J. Yang, Z.M. Jiang, Appl. Phys. Lett. 87 (2005) 223116.
[4] S.W. Lee, P.S. Chen, T.Y. Chien, L.J. Chen, C.T. Chia, C.W. Liu, Thin Solid Films 508 (2006) 120.
[5] B.S. Meyerson, Appl. Phys. Lett. 48 (1986) 797.
[6] P. Meunier-Beillard, M. Caymax, K. Van Nieuwenhuysen, G. Doumen, B. Brijs, M. Hopstaken, L. Geenen, W. Vandervorst, Appl. Surf. Sci. 224 (2004) 31.
[7] M. Stoehr, D. Aubel, S. Juillaguet, J.L. Bischoff, L. Kubler, D. Bolmont, F. Hamdani, B. Fraisse, R. Fourcade, Phys. Rev. B 53 (1996) 6923.
[8] P.H. Tan, K. Brunner, D. Bougeard, G. Abstreiter, Phys. Rev. B 68 (2003) 125302.
[9] M.H. Liao, C.-H. Lee, T.-A. Hung, C.W. Liu, J. Appl. Phys. 102 (2007) 053520.
[10] J.S. Lannin, Phys. Rev. B 16 (1977) 1510.
[11] J.-M. Baribeau, X. Wu, D.J. Lockwood, J. Vac. Sci. Technol. A 24 (2006) 663.
[12] H.T. Johnson, L.B. Freund, J. Appl. Phys. 81 (1997) 6081.
[13] G. Xia, M. Canonico, J.L. Hoyt, International SiGe Technology and Device Meeting (ISTDM), 2006.
[14] E. Rudkevich, F. Liu, D.E. Savage, T.F. Kuech, L. McCaughan, M.G. Lagally, Phys. Rev. Lett. 81 (1998) 3467.
[15] J.-P. Noël, N.L. Rowell, D.C. Houghton, D.D. Perovic, Appl. Phys. Lett. 57 (1990) 1037.
[16] P. Bratu, W. Brenig, A. Groß, M. Hartmann, U. Höfer, P. Kratzer, R. Russ, Phys. Rev. B 54 (1996) 5978.
[17] R. Larciprete, S. Cozzi, E. Masetti, M. Montecchi, G. Padeletti, Thin Solid Films 315 (1998) 49.
[18] A. Nayfeh, C.O. Chui, K.C. Saraswat, T. Yonehara, Appl. Phys. Lett. 85 (2004) 2815.